15

Probing the Dust Obscuration in Seyferts using Infrared Spectroscopy

Joseph H. Rhee & J. E. Larkin

Dept. of Physics and Astronomy,
University of California, Los Angeles

J
KW
NoCa

We present near infrared spectroscopy of 4 Seyfert 1 galaxies, 1 Seyfert 1.9 galaxy, and 1 Seyfert 2 galaxy, obtained using the Gemini infrared camera at the Lick Observatory 3m Shane telescope. With the unique design of the Gemini camera, full J and K band spectra were taken simultaneously through the same slit. This produced a more accurate comparison of hydrogen recombination line fluxes than previous infrared studies. We have also used template galaxies to remove stellar features from the infrared spectra, and produced more accurate measurements of the weak Brγ feature. We concentrate on the velocity resolved ratio of Paβ/Brγ and its implication for dust within the central AGN. For our Seyfert 1's, the line ratios of Paβ/Brγ are not only comparable in both broad and narrow line regions but also consistent with case B recombination confirming that the ratio Paβ/Brγ is less affected by collisional effects than optical lines and is a good indicator of dust extinction up to $A_v \sim 10$ in AGN. Using the same diagnostic the Seyfert 1.9 galaxy, NGC 2992, has an extinction of $A_v = 4.03 \pm 0.20$ to the broad line region while the narrow line region is unobscured. Assuming that Seyfert 1.9 galaxy has the same broad line region that Seyfert 1 galaxies have, we conclude that the obscuring dust is located between the broad line regions and the narrow line regions, consistent with the AGN unification model. The Seyfert 2 galaxy, NGC 5929, consistent with dust being present on larger scales shows significant obscuration to the narrow line region. This data is part of a larger program to measure many spectral properties of Seyfert galaxies.

infrared: galaxy — galaxy: Seyfert — techniques: spectroscopic

Accepted for publication in the July 2000, Vol. 538 # 1, issue of the *Astrophysical Journal*

ABSTRACT

We present near infrared spectroscopy of 4 Seyfert 1 galaxies, 1 Seyfert 1.9 galaxy, and 1 Seyfert 2 galaxy, obtained using the Gemini infrared camera at the Lick Observatory 3m Shane telescope. With the unique design of the Gemini camera, full J and K band spectra were taken simultaneously through the same slit. This produced a more accurate comparison of hydrogen recombination line fluxes than previous infrared studies. We have also used template galaxies to remove stellar features from the infrared spectra, and produced more accurate measurements of the weak Brγ feature. We concentrate on the velocity resolved ratio of Paβ/Brγ and its implication for dust within the central AGN. For our Seyfert 1's, the line ratios of Paβ/Brγ are not only comparable in both broad and narrow line regions but also consistent with case B recombination confirming that the ratio Paβ/Brγ is less affected by collisional effects than optical lines and is a good indicator of dust extinction up to $A_v \sim 10$ in AGN. Using the same diagnostic the Seyfert 1.9 galaxy, NGC 2992, has an extinction of A_v = 4.03±0.20 to the broad line region while the narrow line region is unobscured. Assuming that Seyfert 1.9 galaxy has the same broad line region that Seyfert 1 galaxies have, we conclude that the obscuring dust is located between the broad line regions and the narrow line regions, consistent with the AGN unification model. The Seyfert 2 galaxy, NGC 5929, consistent with dust being present on larger scales shows significant obscuration to the narrow line region. This data is part of a larger program to measure many spectral properties of Seyfert galaxies.

Subject headings: Infrared Spectroscopy, Seyferts, Active Galactic Nuclei

1. Introduction

Active galactic nuclei (AGN) come in a wide variety of forms, but they are typically broken into two general classes based on the presence or absence of very broad (2,000 - 10,000 km/s) emission lines. In the so called Standard Unification theory of Active galactic nuclei, obscuring material is believed to lie between the broad line region and the narrow line region, and the viewing angle toward the broad line region is the only important parameter in determining if an object is seen as a type I AGN (such as Seyfert 1's) or a type II AGN (e.g. Antonucci 1993; Urry & Padovani 1995). In a type I AGN, The line-of-sight is clear of obscuring material toward the broad line region so that we can observe both broad and narrow emission-lines in its spectrum. In a type II AGN, however, optically thick dusty material lies along our line of sight to the broad line region and blocks our view. In a type II AGN only narrow emission lines are detected in its spectrum. Although not without its difficulties, this model does have significant experimental supports. In spectrapolarimetric studies, broad hydrogen recombination lines similar to those in Seyfert 1 galaxies were observed in polarized and scattered light in some Seyfert 2 galaxies (e.g. Antonucci and Miller 1985). An apparent deficit

of ionizing photons (e.g. Wilson, Haniff, & Ward 1988; Kinney et al. 1991; Storchi-Bergmann, Mulchaey, & Wilson 1992) and anisotropic ionization cones around many Seyfert 2 galaxies (e.g. Wilson et al. 1993; Pogge & De Robertis 1993; Wilson & Tsvetanov 1994) have also been used to argue in favor of the unification theory. Some of the strongest evidence of unification comes from Seyfert 2 galaxies that have weak detections of obscured broad hydrogen recombination lines in the infrared.(Goodrich, Veilleux, & Hill 1994; Veilleux, Goodrich, & Hill 1997). There is still a debate, however, if this simple model is the complete answer.

The location of obscuring dust material can be determined by estimating the extinction to both the broad line region and the narrow line region using the ratios of hydrogen recombination lines in different bands. Since infrared emission lines suffer less extinction than similar optical lines, infrared lines are preferred for probing the environment near the nucleus. Some recent infrared studies have given evidence that the broad line regions are considerably more obscured than the narrow-line regions in imtermediate Seyfert galaxies (Veilleux, Goodrich, & Hill 1997; Knop 1997). These studies, however, are often plagued by variable seeing and slit positioning between the different bands as well as contamination from the stellar component from the galaxy. This can lead to different velocity components being present within different spectra and significant variation in flux ratios.

In this paper, we present flux comparisons of Paβ and Brγ both in the narrow line and broad line regions, but also as a function of velocity, within 4 Seyfert 1 galaxies, 1 Seyfert 1.9 galaxy, and 1 Seyfert 2 galaxy. These observations made use of the Gemini twin channel infrared camera at the Lick Observatory. It offers the unique ability to take two broad band spectra simultaneously through the same slit. This greatly reduces variations in slit positioning and seeing, making the line ratios more accurate. This data is part of a larger program to measure many spectral properties of Seyfert galaxies within the infrared.

2. Observations and Reductions

The near-infrared spectra were taken using the Gemini twin channel infrared camera at the Lick Observatory 3m Shane telescope during April, 1998. For all observations, Grisms with a resolution of ~550 were used for both the J and K bands. The large wavelength coverage (e.g. 1.09 μm to 1.39 μ for J band and 1.96 μm to 2.4 μm for K band) of the Gemini grisms included the redshifted Paβ ($\lambda = 1.2818$ μm) and Brγ ($\lambda = 2.1655$ μm) lines as well as HeI ($\lambda = 1.08$ μm), FeII ($\lambda = 1.256$ μm), H_2 ($\lambda = 2.122$ μm) and the CO bandheads ($\lambda = 2.29+$ μm). The entrance slit has a fixed width of 2 pixels (1.2") and a fixed N-S orientation. The unique design of the Gemini camera takes both J and K bands spectra into the same slit simultaneously, greatly reducing variations in slit positioning and seeing.

In order to center the objects on the slit, J, H, & K band images were taken first, and the telescope was moved to place the centroids of the galaxy nucleus on the slit center. The images

were used later to flux-calibrate the galaxy spectra. For each object, the galaxy was moved back and forth along the slit by 1' in order that one spectrum in each pair could be used as the sky frame of the other spectrum. Each individual exposure was typically 600 seconds long. The summary of our observations is given in Table 1.

Main-sequence G stars selected from the Yale Bright Star Catalog (Hoffleit D. 1964) were observed before and after the galaxy to remove telluric absorption from the galaxy spectra and to serve as flat fields. We divided each star by a solar spectrum which had previously had its black body slope removed in order to remove most of the weak stellar features. Some residuals of Paβ and Brγ still remained due to different spectral types and were removed by interpolation. In the infrared, stellar absorption features in main-sequence G stars are not as significant as in the optical. The equivalent widths of Paβ and Brγ are just ~ 2 $\AA$ (see Appendix in Larkin 1996). The redshifts of the galaxies ($>$ 900 km/s, except for NGC 4569) should leave the galactic spectra unaffected by any contamination from interpolation over Paβ and Brγ.

For the galaxies, first, image pairs were subtracted. Then the interpolated star frames were used to divide the galaxy frames. Bad pixels were replaced by the median of their neighboring pixels. Atmospheric OH emission lines in the stellar spectrum were fitted with second-order polynomials in order to rectify the spectral lines in wavelength and spatial extent. Wavelengths for the OH lines were obtained from Oliva & Origlia (1992)

An HST infrared standard star was also observed at J and K bands to flux-calibrate the images. A 2x8 pixel synthetic aperture centered on the nucleus of broad band images was used to determine the magnitudes inside the slit for each galaxy spectrum. Using the absolute flux density at zero magnitude (Koornneef 1983), flux density in each spectrum was obtained to scale the counts to actual flux.

After correction of atmospheric absorption and flux calibration, the intensities of Paβ and Brγ were measured from the broad band spectra for each galaxy. This procedure was done in two parts. First, we used the spectrum of a template galaxy to fit a continuum below each emission line to correct the underlying stellar absorption features in the galaxy spectra. We employed the spectrum of NGC 3115 to fit J band continuum and NGC 5557 for K band continuum. Previous studies found that underlying stellar absorption features were one of the main difficulties in measuring accurate hydrogen line ratios (see e.g. Rix, Carleton, Rieke, & Rieke 1990; Veilleux, Goodrich, & Hill 1997; Larkin et al. 1998). The wavelength of the template galaxy was multiplied by the ratio of redshifts (e.g. $(1+z)_{galaxy}/(1+z)_{template}$)to match the Seyfert galaxy of interest. The ratio of the photon counts per pixel of the template galaxy to that of the target galaxy was then multiplied to the spectrum of template galaxy to match the continuum of the target galaxy. By subtracting the corrected template spectrum from the galaxy spectrum, we obtained emission-only spectrum for each galaxy. Although we believe that neither galaxy serves as a perfect template for our target galaxies, these galaxies provide more accurate baselines than simple linear fits. For example, in the J band, our template galaxy, NGC 3115, removes unknown bumps between FeII line and Paβ line

and recovers missing features in the extended right wing of Paβ which are consistent in most of our target galaxies. The second step was to fit the continuum-subtracted emission lines with Gaussians. We first fitted the broad line components with a Gaussian excluding the central region. The best fits to the broad line components were then subtracted from the emission lines so that the remaining narrow line components could be fitted with a Gaussian also. Since the broad line components of Paβ and Brγ were typically non-Gaussian, only the Gaussian fits to the narrow line components were used to calculate the narrow line fluxes while the remaining broad line emission was integrated to get the broad line fluxes. For NGC 3516 and NGC 5548, their broad lines completely dominate the spectrum, so no narrow line component could be determined. For those two objects, we used their total flux to represent their broad line strengths.

3. Results

The spectra of 4 Seyfert 1 galaxies, 1 Seyfert 1.9 galaxy and 1 Seyfert 2 galaxy are presented in Figure 1 and 2. Three Seyfert 2 galaxies were orginally observed; however, only one of these galaxies is presented due to the absence of strong features and very low signal to noise ratio in NGC 3362 and NGC 4569. The top panel of each set shows the J band spectrum in which FeII (λ = 1.2567 μm) and Paβ (λ = 1.2818 μm) are the dominant emission lines. The bottom panel depicts the K band spectrum in which H_2 line (λ = 2.1218 μm) and Brγ line (λ = 2.166) typically stand out. The featureless spectra of the template galaxies (NGC 3115 for J band and NGC 5557 for K band) serve as continua for all the galaxy spectra and are shown in a dotted line. The process of fitting the continuum contributed the most to the uncertainty of flux calibration of Paβ and Brγ. All the emission lines in the Figures are shown at their redshifted wavelengths; for example, Paβ line in NGC 3227 appears at 1.2867 μm.

Figures 3 and 4 show the continuum-subtracted emission features of Paβ and Brγ for each galaxy. The dotted lines show the narrow-line-subtracted tops of the broad line components while the gaussian curves at the bottom depict the narrow line components. NGC 3516 and NGC 5548 were not fit with gaussian curves at all.

Total fluxes of the Paβ and Brγ lines and their flux ratios are tabulated in Table 2. The tabulated fluxes and ratios include the uncertainty in the flux calibration at each wavelength. The total flux ratio of Paβ/Brγ in Seyfert 1 galaxies ($\sim$ 6) is greater than those of both Seyfert 1.9 and Seyfert 2 galaxies ($\sim$ 3) in general. Table 3 lists the total flux and Paβ/Brγ ratios for the narrow line component in each galaxy as Table 4 does for the broad line component. All four Seyfert 1 galaxies in our sample show comparable line ratios of Paβ/Brγ close to 6 in both broad and narrow line components. These ratios are consistent with case B recombination and no extinction. In the intermediate Seyfert galaxy, NGC 2992, the narrow line ratio is comparable with those from Seyfert 1's (i.e. Paβ/Brγ is $\sim$ 6) while the broad line ratio is down by a factor of 2. These ratios imply that the obscuring material affects the broad line region but not the narrow line region. The

Seyfert 2 galaxy, NGC 5929, however, shows a narrow line ratio significantly lower than those from the Seyfert 1's.

Listed in column (6) in Table 3 and 4 are visual extinctions for the narrow line regions and the broad line regions in our sample of galaxies. The intrinsic line ratio of Paβ/Brγ was obtained from an average value of case B recombination ratios (i.e. 6.01±0.22) for hydrogen given in Osterbrock (1989) for the calculation.

4. Discussion

Our results for a sample of Seyfert 1's show that flux ratios of Paβ and Brγ are close to 6 in both narrow and broad line regions(see Tables 3 and 4). These flux ratios are consistent with case B recombination ratios for hydrogen with no obscuration. Although case B has been applied to optically thin narrow line regions, its application to the broad line regions has been questionable due to possible collisional effects (Osterbrock 1989, Peterson 1997). They don't, however, seem to affect our data significantly, possibly because Paβ(n = 5 to n = 3) and Brγ(n = 7 to n = 4) are higher level transitions and are less affected by collisions. A similar conclusion was reached by Hill et al. in their infrared spectroscopic study of radio galaxies as they reported that their observed line ratios of high level transitions were consistent with case B in quasar, 3CR 273 (see Table 6 in Hill et al. 1996). Recently N. Murray and his collegues have developed a new model for the structure of the broad line region (1995). In their model, a wind is driven off the accretion disk, and this wind produces the broad emission line spectrum as well as the absorption trough in BAL objects. According to the discussion of the Balmer lines in their papers, Paβ and Brγ would need to be optically thin and therefore double-peaked in the line profile (Murray N. &. Chiang J. 1997). Our lines, however, show single-peaked profiles and some mechanism other than that discussed in the paper must be found. The only other possibility is that some other component fills in the core and leaves the profile smooth and single-peaked as observed. The pertinency of case B ratio to both the narrow and broad line regions as well as the penetrating powers of infrared lines upto $A_v \sim 10$ makes the line ratio of Paβ/Brγ a useful diagnostic tool of central obscuration. Visual extinction determined using case B indicates almost no extinction by dust toward both the narrow line regions and the broad line regions in our sample of Seyfert 1's. All four of our objects (e.g. NGC 3227, NGC 3516, NGC 4151, & NGC 5548) are included in the recent optical spectroscopic study conducted by Ho et al. in 1997 (see Table 4). The narrow line extinctions in both surveys are in agreement with each other. This result upholds this aspect of the standard AGN unification model, in which observers have an unobscured view of the broad line region in a type I AGN.

NGC 2992 is classified as a Seyfert 1.9 galaxy and has both broad and narrow line regions. The ratio Paβ/Brγ is 6.05±2.19 in the narrow line region and 3.73±0.78 in the broad line region consistent with extinction by dust in the broad line region only. Since NGC 2992 is highly inclined, obscuration to the broad line region might also come from dust in the host galaxy plane rather than the nuclear torus (see e.g. Antonucci 1993 Sec. 2.2). If NGC 2992 is obscured by dust in the host

galaxy plane, we might expect comparable extinction from both the narrow and broad line regions. Our data, however, show extinction to the broad line regions only; therefore, the broad line region in NGC 2992 is obscured by nuclear dust. The larger extinction to the broad line region places the obscuring dust between the narrow line region and the broad line region. Infrared spectroscopic studies by Veilluex et al. (1997) on intermediate Seyfert galaxies and by Hill et al. (1996) on radio galaxies have reached the same conclusion.

In Table 4, the Seyfert 2 galaxy NGC 5929 has a flux ratio far lower than 6 for Paβ/Brγ in the narrow line region. NGC 5929 is very strongly interacting with its companion NGC 5930 (De Robertis, Yee, & Hayhoe 1998). A low flux ratio of Paβ over Brγ, hence high extinction, is perhaps caused by dust from the interacting system, not from the nuclear torus. The spectrum of NGC 3362 is very noisy due to low signal to noise ratio resulting in a large uncertainty in flux ratio. Both Paβ and Brγ were undetected in NGC 4569. With the data from NGC 5929 alone, it is, therefore, very difficult to apply this ratio to all Seyfert 2 galaxies. NGC 5929 might be just one peculiar object with dust on the large scales. We clearly need a larger sample of Seyfert 2 galaxies to draw any more significant conclusions.

5. Summary and Conclusions

We have presented the flux ratios of hydrogen recombination lines in the infrared in both Seyfert 1 and Seyfert 2 galaxies. We have made use of template galaxies in the infrared to remove stellar features that contaminate the AGN spectra. This has enabled us to accurately measure fluxes for weak broad emission lines. We conclude the following from our data:

1. We find that for Seyfert 1's the spectra are consistent with case B recombination with little obscuration.

2. The pertinency of case B ratio to the both narrow and broad line regions as well as the penetrating powers of infrared lines up to $A_v \sim 10$ makes the line ratio of Paβ/Brγ a useful diagnostic tool of central obscuration.

3. Our results show no extinction in Seyfert 1 galaxies and partial extinction to only the broad line region in a Seyfert 1.9 galaxy which are consistent with the standard AGN unification model.

4. Only one of our Seyfert 2 galaxies had sufficient signal-to-noise for similar comparison, but it had an relatively high level of obscuration and suggested dust on large scales.

We have taken an additional set of both Seyfert 1 and Seyfert 2 galaxies in the end of December 1998, and this set will help us to draw more complete diagnosis on the unified AGN model in the future.

We thank the Lick observatory staffs and especially our night assistant, Kostas Chloros. We also like to thank Jonah Hare for helping with observation. We thank our referee, R. Antonucci for his very helpful comments and suggestions on this paper.

REFERENCES

Antonucci, R 1993, ARAA, 31, 473
Antonucci, R. R. J., & Miller, J. S. 1985, ApJ, 297, 621
De Robertis, M. M., Yee, H. K., & Hayhoe, K. 1998, ApJ, 496, 93
Hoffleit, D. 1964, Catalogue of Bright Stars, Yale University Observatory, Third Revised Edition
Goodrich, R. W., Veilleux. S., & Hill, G. J. 1994, ApJ, 422, 521
Hill, G. J., Goodrich, R. W., & DePoy, D. L. 1996, ApJ, 462, 163
Ho, Luis C., Filippenko, Alexei V., & Sargent, Wallace L. W. 1997, ApJS, 112, 315
Kinney, A. L., Antonucci, R. R. J., Ward, M. J., Wilson, A. S., & Whittle, M. 1991, ApJ, 337, 100
Knop Jr., R. A. 1997, PhD thesis, Caltech
Koornneef, J. 1993, A&A, 128, 84
Larkin, J. E., Armus, L., Knop, R. A., Soifer, B. T., & Matthews, K. 1998, ApJS, 114, 59L
Larkin, J. E. 1996, PhD thesis, Caltech
Murray, N., Chiang J. 1997, ApJ, 474, 91
Murray, N., Chiang J., Grossman, S. A., & Voit, G. M. 1995, ApJ, 451, 498
Osterbrock, D. E., 1989, Astrophysics of Gaseous Nebulae and Active Galactic Nuclei, University Science Books
Peterson, B. M., 1997, An Introduction to active galactic nuclei, Cambridge University Press
Pogge, R. W., & De Robertis, M. M. 1993, ApJ, 404, 563
Rix, H., Carleton, N. P., Rieke, G., & Rieke, M. 1990, ApJ, 363, 48
Storchi-Bergmann, T., Mulchaey, J. S., & Wilson, A. S. 1992, ApJ, 395, L73
Urry, C. M., & Padovani, P. 1995, PASP, 107, 803
Veilleux, S., Goodrich, R. W., & Hill, G. J. 1997, ApJ, 477, 631
Wilson, A. S., Braatz, J. A., Heckman, T. M., Krolick, J. H., & Miley, G. K. 1993, ApJ, 419, L61
Wilson, A. S., Haniff, C. A., & Ward, M. J. 1998, ApJ, 334, 121 Wilson, A. S., & Tsvetanov, Z. I. 1994, AJ, 107, 1227

This preprint was prepared with the AAS LaTeX macros v5.0.

TABLE 1
Observation Summary

Object	Type	1+z	Integration time (min)
NGC 3227	S1.5	1.00382	30
NGC 3516	S1	1.00875	20
NGC 4151	S1	1.00319	30
NGC 5548	S1	1.01675	30
NGC 2992	S1.9	1.00778	30
NGC 3362	S2	1.02774	15
NGC 4569	S2	0.99896	30
NGC 5929	S2	1.00838	30
NGC 3115	template	1.00223	15
NGC 5557	template	1.01065	20

TABLE 2
Total Fluxes of Paβ and Brγ

Object	Type	Paβ flux	Brγ flux	Paβ/Brγ
		erg/cm^2/s		
NGC 3227	S1.5	(1.82±0.24)E-13	(3.02±0.30)E-14	6.03±1.00
NGC 3516	S1	(2.13±0.33)E-13	(3.61±0.54)E-14	5.90±1.27
NGC 4151	S1	(1.06±0.11)E-12	(1.67±0.18)E-13	6.35±0.93
NGC 5548	S1	(1.42±0.15)E-13	(2.43±0.36)E-14	5.85±1.07
NGC 2992	S1.9	(7.41±1.18)E-14	(1.89±0.22)E-14	3.92±0.78
NGC 3362	S2	...	...	...
NGC 4569	S2	...	...	...
NGC 5929	S2	(2.99±0.40)E-14	(9.60±1.37)E-15	3.11±0.62

TABLE 3
Total Fluxes of Narrow line Components

Object	Type	Paβ flux	Brγ flux	Paβ/Brγ	A_v
		erg/cm^2/s			
NGC 3227	S1.5	(2.54±0.45)E-14	(4.20±0.96)E-15	6.05±1.76	-0.05±0.17
NGC 3516	S1	...	...	...	...
NGC 4151	S1	(10.4±0.90)E-14	(1.62±0.20)E-14	6.44±0.98	-0.51±0.12
NGC 5548	S1	...	...	...	...
NGC 2992	S1.9	(1.93±0.26)E-14	(3.11±0.63)E-15	6.19±1.50	-0.21±0.15
NGC 3362	S2	...	...	...	...
NGC 4569	S2	...	...	...	...
NGC 5929	S2	(3.08±0.36)E-14	(9.60±1.30)E-15	3.21±0.57	4.61±0.19

TABLE 4
Total Fluxes of Broad line Components

Object	Type	Paβ flux	Brγ flux	Paβ/Brγ	A_v
		erg/cm^2/s			
NGC 3227	S1.5	(1.57±0.22)E-13	(2.60±0.28)E-14	6.03±1.06	-0.02±0.13
NGC 3516	S1	(2.13±0.33)E-13	(3.61±0.54)E-14	5.90±1.27	0.14±0.15
NGC 4151	S1	(9.60±1.03)E-13	(1.51±0.18)E-13	6.35±0.93	-0.41±0.26
NGC 5548	S1	(1.42±0.15)E-13	(2.43±0.36)E-14	5.85±1.07	0.19±0.14
NGC 2992	S1.9	(5.48±1.00)E-14	(1.58±0.15)E-14	3.47±0.71	4.03±0.20
NGC 3362	S2	...	...	...	...
NGC 4569	S2	...	...	...	...
NGC 5929	S2	...	...	...	...

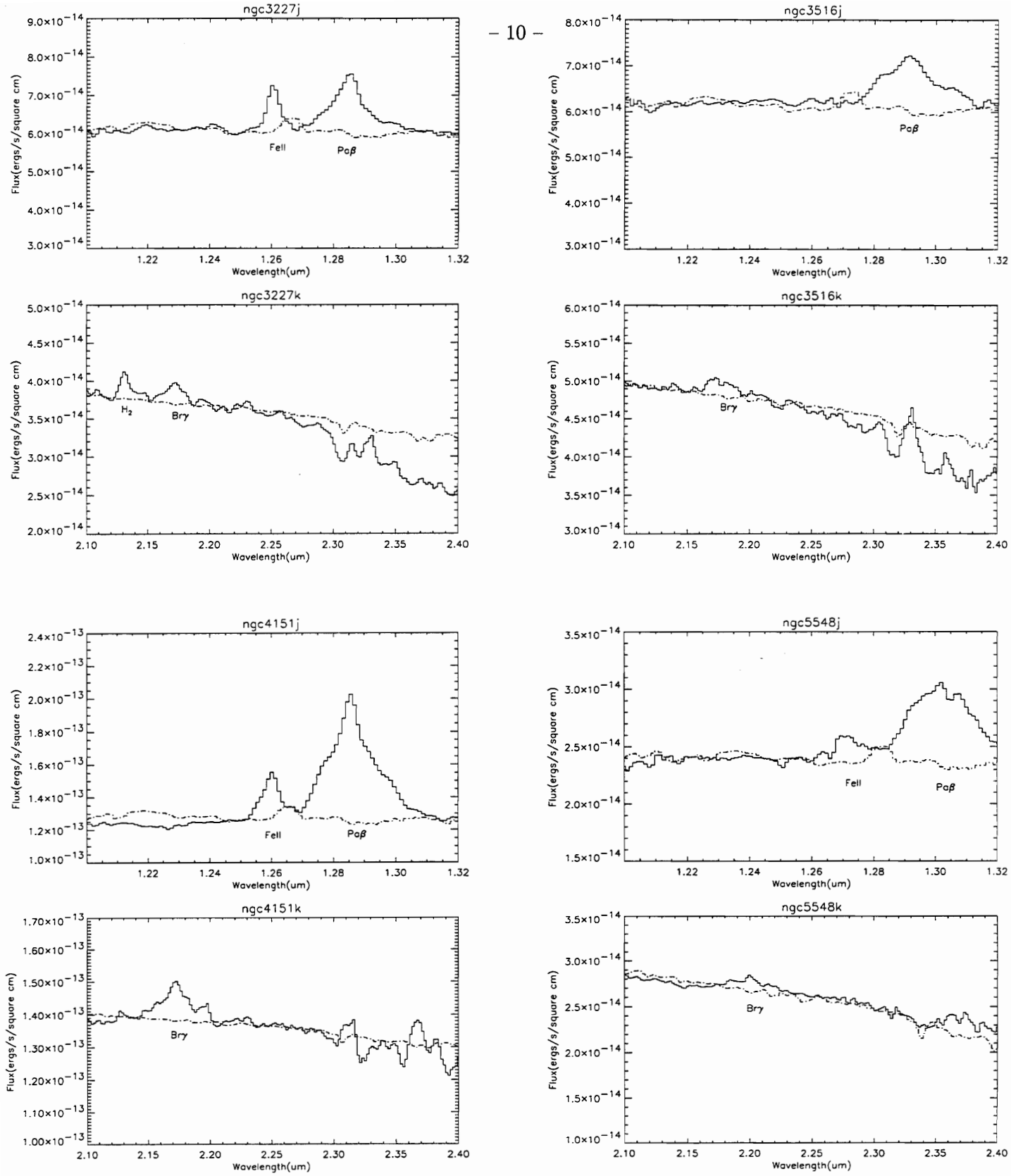

Fig. 1.— The spectra of 4 Seyfert 1 galaxies. In each set, the top panel represents J band specrtrum and the bottom panel K band spectrum. The template galaxy is shown in a dotted line in every set.

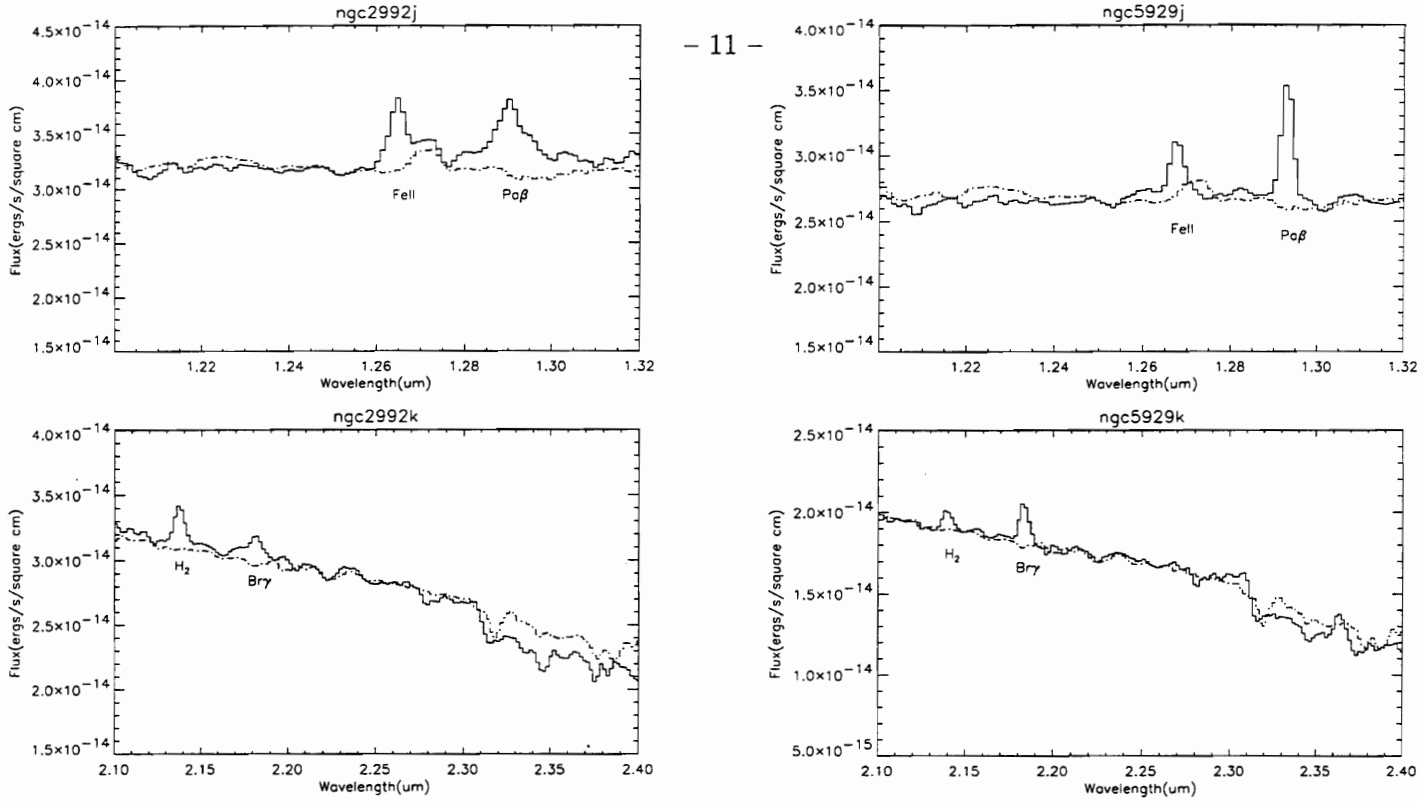

Fig. 2.— The spectra of the Seyfert 1.9 galaxy, NGC 2992 and Seyfert 2 galaxy, NGC 5929. In each set, the top panel represents J band specrtrum and the bottom panel K band spectrum. The template galaxy is shown in a dotted line in every set.

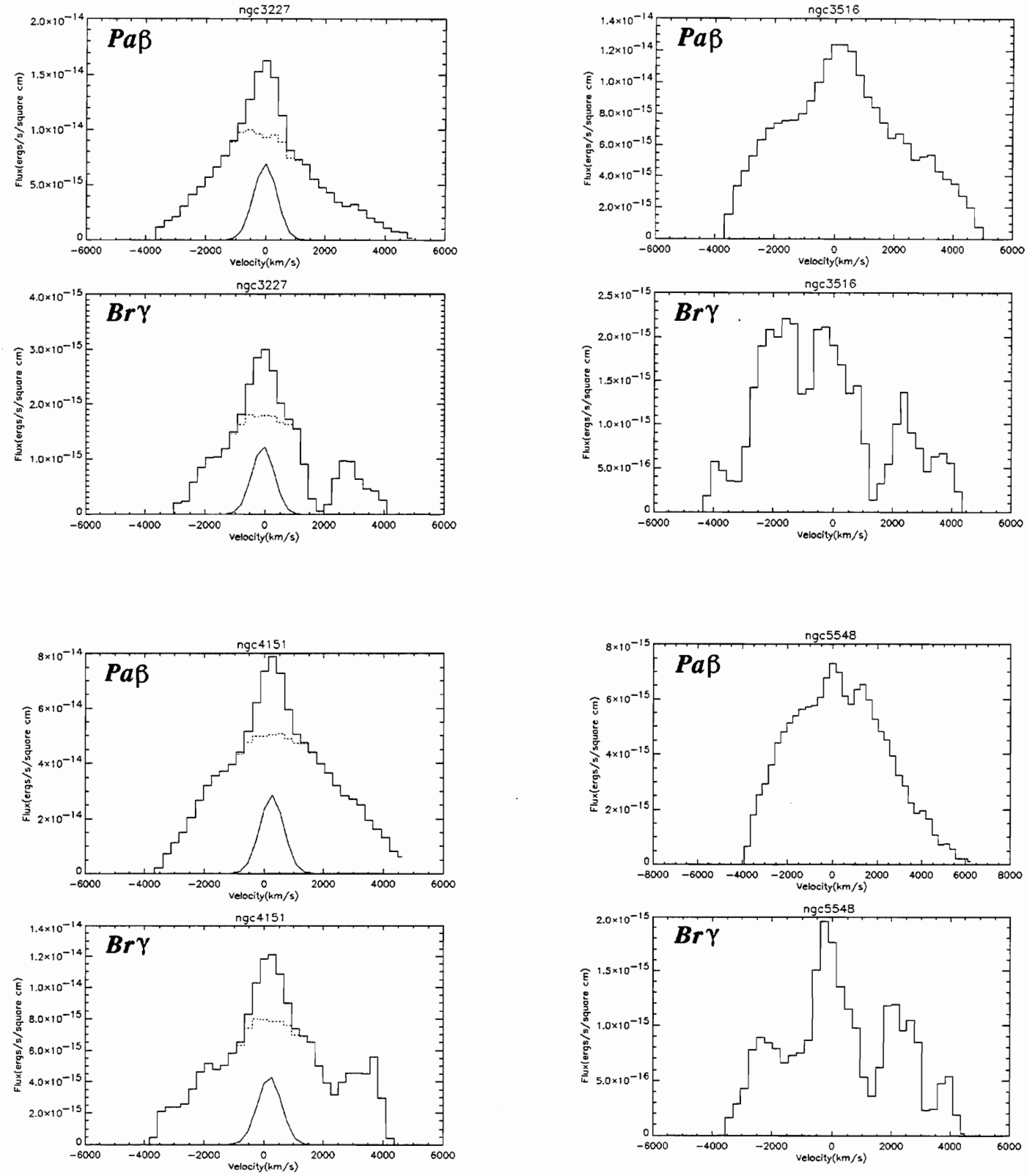

Fig. 3.— The continuum-subtracted spectra of 4 Seyfert 1 galaxies. The x-axis is shown in relative velocity and the y-axis in flux. The dotted lines represent the narrow-line-subtracted tops of broad line component while the gaussian curves at the bottom depict the narrow line components

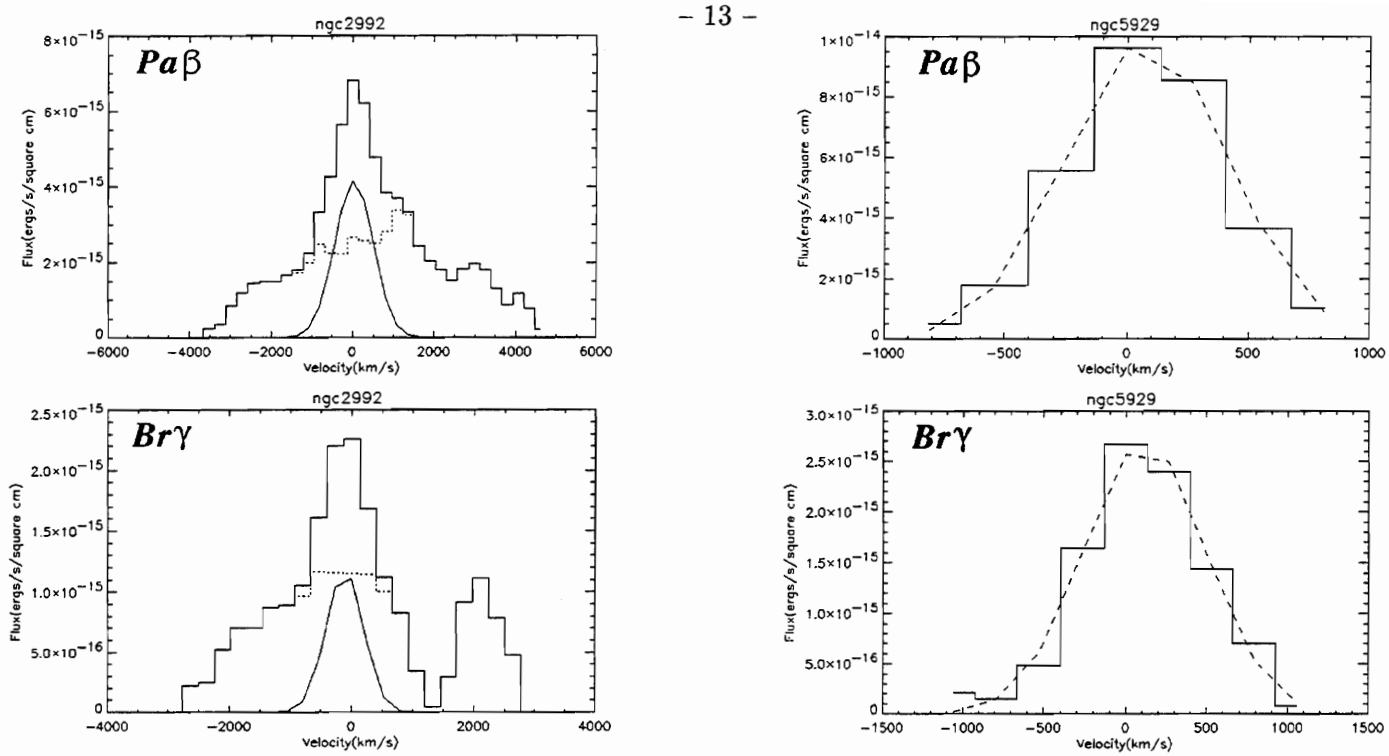

Fig. 4.— The continuum-subtracted spectra of the Seyfert 1.9 galaxy, NGC 2992 and Seyfert 2 galaxy, NGC 5929. The x-axis is shown in relative velocity and the y-axis in flux. The dotted line represents the narrow-line-subtracted top of broad line component while the gaussian curve at the bottom depicts the narrow line component in NGC 2992. For a Seyfert 2 galaxy, NGC 5929, the narrow line components were fit with Gaussian curves which are shown in dotted line